5-30-2022

PAHs in the North Atlantic Ocean and the Arctic Ocean: Spatial Distribution and Water Mass Transport

Mengyang Liu

Minggang Cai

Mengshan Duan

Meng Chen

Rainer Lohmann

See next page for additional authors

Authors

Mengyang Liu, Minggang Cai, Mengshan Duan, Meng Chen, Rainer Lohmann, Yan Lin, Junhua Liang, Hongwei Ke, and Kai Zhang

PAHs in the North Atlantic Ocean and the Arctic Ocean: Spatial Distribution and Water Mass Transport

Mengyang Liu[1,2,3], Minggang Cai[1,3,*], Mengshan Duan[3], Meng Chen[4], Rainer Lohmann[5], Yan Lin[3,6], Junhua Liang[3], Hongwei Ke[3], Kai Zhang[2]

[1]State Key Laboratory of Marine Environmental Science, Xiamen University, Xiamen 361102, China

[2]State Key Laboratory of Marine Pollution, City University of Hong Kong, Hong Kong 999077, China

[3]College of Ocean and Earth Sciences, Xiamen University, Xiamen 361102, China

[4]College of the Environment and Ecology, Xiamen University, Xiamen 361102, China

[5]Graduate School of Oceanography, University of Rhode Island, Narragansett, RI 02882, USA

[6]College of the Environmental Science and Engineering, Xiamen University of Technology, Xiamen 361002, China

Corresponding author: Minggang Cai, mgcai@xmu.edu.cn

Key Points:

- PAHs showed an "Arctic Shelf > Atlantic Ocean > Arctic Basin" distribution pattern.
- The net transport flux of PAHs was 63 ± 53 tons year^{-1} to the Arctic Ocean.
- Ocean current was a less-dominant pathway for PAHs entering the Arctic Ocean.

Abstract

In the Arctic Ocean, it is still unclear what role oceanic transport plays in the fate of semivolatile organic compounds (SVOCs). The strong-stratified Arctic Ocean undergoes complex inputs and outputs of polycyclic aromatic hydrocarbons (PAHs) from the neighboring oceans and continents. To better understand PAHs' transport processes and their contribution to high-latitude oceans, surface seawater, and water column samples were collected from the North Atlantic Ocean and the Arctic Ocean in 2012. The spatial distribution of dissolved PAHs ($\sum_9$PAH) in surface seawater showed an "Arctic Shelf > Atlantic Ocean > Arctic Basin" pattern, with a range of 0.3–10.2 ng L^{-1}. Positive matrix factorization (PMF) modeling results suggested that vehicle emissions and biomass combustion were the major PAHs sources in the surface seawater. According to principal component analysis (PCA), PAHs in different water masses showed unique profiles indicating their different origins. Carried by the Norwegian Atlantic Current (0–800 m) and East Greenland Current (0–300 m), PAH individuals' net transport mass fluxes ranged from -4.4 ± 1.7 to 53 ± 39 tons $year^{-1}$ to the Arctic Ocean. We suggested the limited contribution of ocean currents on PAHs' delivery to the Arctic Ocean, but their role in modulating PAHs' air-sea interactions and other biogeochemical processes needs further studies.

Plain Language Summary

Organic pollutants could transport between the Arctic Ocean and the neighboring oceans through ocean currents, and their marine fates are still unclear. Polycyclic aromatic hydrocarbons (PAHs) are a class of semivolatile organic compounds with ongoing emissions from petrogenic and pyrogenic sources. We analyzed dissolved PAHs in seawater collected from the North Atlantic Ocean and the Arctic Ocean, founding their distribution showing an "Arctic Shelf > Atlantic Ocean > Arctic Basin" pattern. PAHs in the surface seawater probably came from vehicle emissions and biomass combustion, and their unique profiles indicated their different origins in deep water masses. We estimated the transport of PAHs within the Norwegian Atlantic Current (0–800 m) and East Greenland Current (0–300 m), finding the net poleward flows of PAH individuals ranging from -4.4 ± 1.7 to 53 ± 39 tons $year^{-1}$. This study suggested a limited contribution of ocean currents on PAHs' physical transport, but further investigations should consider their indirect impact on their marine fates.

1 Introduction

The Arctic Ocean, linking the Atlantic Ocean and the Pacific Ocean, is a fundamental node in the global hydrological cycle and thermohaline circulation (Talley et al., 2011; Carmack et al., 2016). A major inflow to the Arctic Ocean comes from the Atlantic through the Fram Strait and the Barents Sea, with a minor inflow from the Pacific side through Bering Strait (Ma et al., 2018; Liu et al., 2021a). The outflow from the Arctic Ocean, being cold and fresh, is mainly conveyed by East Greenland Current through the Fram Strait, which is the only deep channel allowing energy and materials to exchange between the Arctic Ocean and other oceans (Wang et al., 2021). The Arctic is the most sensitive area worldwide and is undergoing

visible and less visible changes such as warming, refreshing, and sea ice loss (Morison et al., 2012; Dai et al., 2019; Ko et al., 2020). External to the Arctic Ocean, the bordering subarctic oceans are undergoing substantial changes in heat, salt, and biogeochemical properties, therefore amplifying the climate response of the Arctic Ocean (Steele and Boyd, 1999).

Semivolatile organic compounds (SVOCs) exist in the environments ubiquitously (Lohmann et al., 2007; Hung et al., 2010; Xue et al., 2016). Among them, polycyclic aromatic hydrocarbons (PAHs) are of great concern because of their toxicity or carcinogenic effects and the ongoing emissions from pyrogenic or petrogenic sources (Shen et al., 2013; Balmer et al., 2019; Du et al., 2020; Wang et al., 2020). Similar to persistent organic pollutants (POPs) with long-range transport potential, PAHs could arrive in the Arctic Ocean through the atmospheric or oceanic pathway, but their fate remains unclear (Ma et al., 2013; Liu et al., 2021a). On the one hand, climate changes may lead to PAHs' re-volatilization from the Arctic (Nizzetto et al., 2010; Yu et al., 2019). On the other hand, their biogeochemical processes, e.g., biodegradation, photodegradation, and vertical sinking, would be further impacted due to the changes in temperature, light, and degrader species (Keyte et al., 2013; Deyme et al., 2011; González-Gaya et al., 2019). Hence, it is challenging but necessary to better understand the transport and fate in the changing Arctic.

Hydrological processes, such as ocean current transport, would make a crucial contribution to the long-range transport of POPs, especially in the deep ocean (Lohmann and Belkin, 2014). Inflowing Atlantic and Pacific waters eventually flow out to the North Atlantic after experiencing cooling and freshwater input in the Arctic Ocean; thus, the pollutants in the Arctic Ocean are likely to be transported via ocean currents on a larger ocean scale (Carmack et al., 2016). According to the limited studies, the outflows of hexachlorocyclohexanes (HCHs) and hexachlorobenzene (HCB) are detected in the deep waters from the Arctic Ocean through Fram Strait, while polychlorinated biphenyls (PCBs) are still loaded from the Atlantic Ocean to the Arctic Ocean (Ma et al., 2018). The previous study has suggested the Atlantic meridional overturning circulation and deep ocean transport reduce perfluorooctane sulfonate (PFOS) accumulated in the Arctic Ocean (Zhang et al., 2017). For the non-volatile perfluorooctanoic acid (PFOA), oceanic transport would make a more significant contribution to pollutants in the Arctic (Stemmler and Lammel, 2010). Those results all implied that oceanic transport in the deep ocean is important for their distribution and storage. However, for POPs with different emission trends, it is unclear whether their export from the Arctic Ocean via ocean currents exceeds their input, or whether the Arctic Ocean is still a net sink for pollutants (Sobek and Gustafsson, 2014).

Oceanic transport of POPs is not only a physical mixing process, but also probably influences their biogeochemical processes, such as biodegradation and particulate settling, by changing temperature, dissolved oxygen, and seawater nutrients (Liu et al., 2021b). The strong-stratified Arctic Ocean undergoes complex inputs and outputs of PAHs from the neighboring oceans and continents. The upper

ocean plays a crucial role in transporting PAHs from the surface to their major sinks. To better understand PAHs' transport processes and their contribution to high-latitude oceans, we investigated surface seawater and water-column samples in the North Atlantic Ocean and the Arctic Ocean. The objectives of this study were (i) to obtain broad-scale spatial distributions and sources of PAHs in the surface seawater of the North Atlantic and the Arctic Ocean, (ii) to obtain the vertical profiles of PAHs in different water masses and investigate the potential biogeochemical influences, (iii) to estimate mass flows of PAHs between the North Atlantic and the Arctic Ocean, and to evaluate the role of oceanic transport in PAHs' cycling.

2 Materials and Methods

2.1 Sample collection

Samples were conducted in the Arctic (Canada Basin, Amundsen Basin, East Siberian Sea, and Barents Sea) and the North Atlantic (Iceland Sea, Greenland Sea, and Norwegian Sea) during the 5th Chinese National Arctic Research Expedition between July and September 2012, onboard *RV Xuelong* (Figure 1). Surface seawater samples were taken from 18 sites, and in addition, water-column samples were taken from four sites (AT06, BB04, IS02, and SR18). These four sites were located in different areas with different hydrodynamics and bottom depths (821–3409 m), as AT06 and BB04 were in the Norwegian Sea, IS02 in the Greenland Sea, and SR18 in the central Arctic. Details of the sampling sites are shown in the Supporting Information in Table S1, and the sampling volume for each sample was approximate 4 L. Briefly, surface seawater samples were collected using the vessel's seawater intake system (stainless steel pipe), and water-column samples were collected in Niskin bottles mounted on a CTD rosette (Seabird 911/17) at multiple layers. The collected samples were immediately filtered through a pre-combusted (450^{o}C, 4 h) Whatman glass microfiber filter (GF/F; 47 mm diameter, 0.7μm pore size) and stored in amber glass bottles. The solid-phase extraction (SPE) C_{18} cartridges were pre-cleaned with dichloromethane, followed by acetone and hexane on land, and were pre-conditioned with methanol followed by ultrapure water onboard. Spiked with surrogate standards (acenaphthylene-d10, phenanthrene-d10, chrysene-d12, and perylene-d12), the filtrate was passed through pre-conditioned cartridges at a flow rate of 6 mL min^{-1}. After the extraction, the cartridges were well wrapped with pre-combusted aluminum foil and stored at −20°C until sample pretreatment.

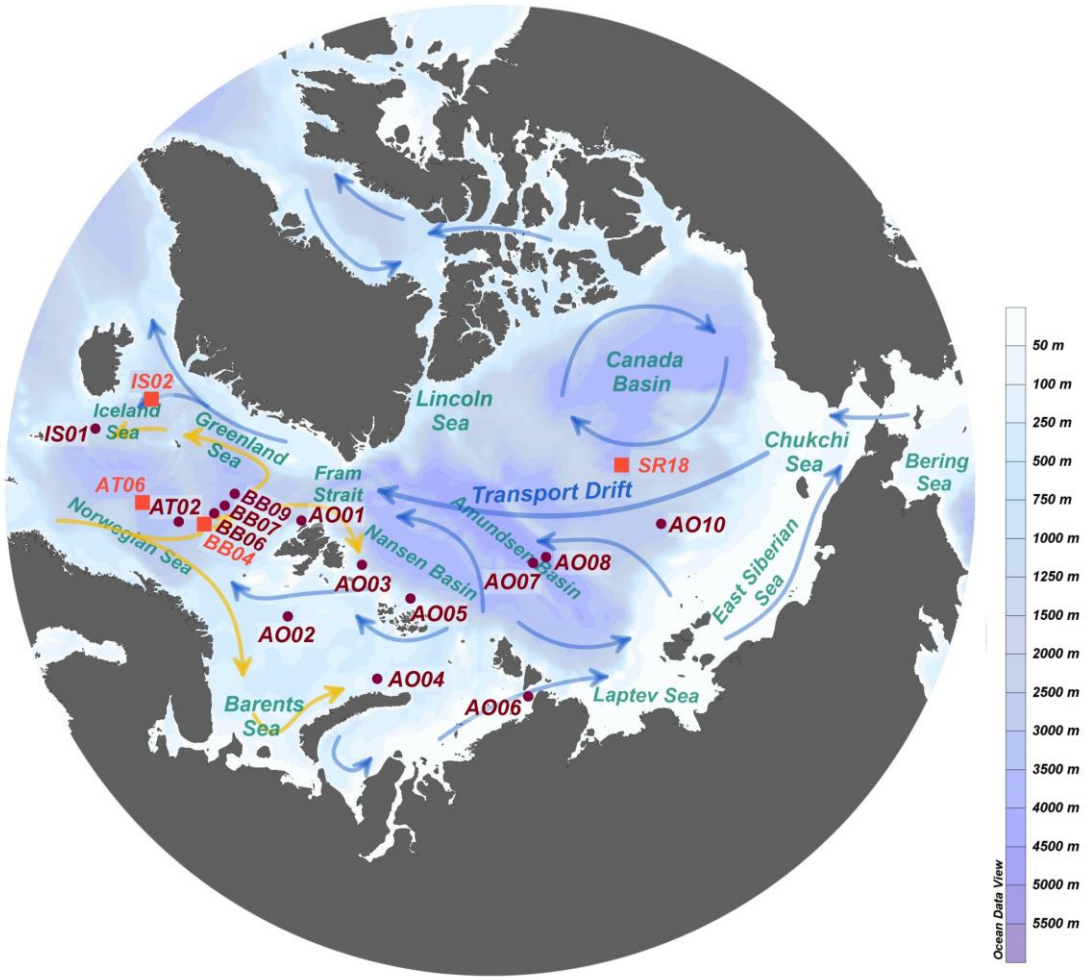

Figure 1. Locations of sampling sites for seawater samples in the North Atlantic Ocean and the Arctic Ocean. The dark red dots represent sites for surface seawater samples, and the bright red squares represent sites for water-column samples.

2.2 Pretreatment and instrumental analysis

The pretreatment for dissolved PAHs was conducted as described earlier (Liu et al., 2021a). In brief, for dissolved PAHs, SPE cartridges were eluted with 10 mL of ethyl acetate and anhydrated by pre-combusted anhydrous sodium sulfate. The eluents were solvent-exchanged to n-hexane and concentrated to 1 mL using a rotary evaporator. After further evaporation under a gentle nitrogen stream, the mixture was spiked with 5 ng of internal standard (pyrene-d10), and stored at −4°C before the instrumental analysis. 16 USEPA priority PAHs were analyzed by gas chromatography coupled with double mass spectrometry (GC-MS-MS, Agilent 7890A-7000B). Details of the instrumental analysis are shown in Text S1.

158 ### 2.3 QA/QC

159 Field blanks, lab blanks, and spiked surrogates were performed to control data
160 quality. Each field blank (Table S3) was performed using 4 L of distilled water and
161 shared the same treatment from storage in an amber glass bottle and filtration to the
162 final instrumental analysis. Laboratory blanks (Table S3) were performed on cleaned
163 SPE C_{18} cartridges in the same manner as the laboratory samples to prevent any
164 contamination originating from the described experimental processes. Instrumental
165 detection limits and the ions monitored are shown in Table S2. Among the 16 USEPA
166 PAHs analyzed here, 10 PAHs showed detectable concentrations, namely,
167 naphthalene (Nap), acenaphthylene (Acpy), acenaphthene (Acp), fluorene (Flu),
168 phenanthrene (Phe), anthracene (Ant), fluoranthene (FluA), pyrene (Pyr),
169 benzo(a)anthracene (BaA), and chrysene (Chr). Method detection limits were derived
170 from the mean field blanks plus three times the standard deviation of the field blanks,
171 and ranged from <0.01 ng L^{-1} (Chr) to 4.30 L^{-1} (Nap), as shown in Table S3. Nap
172 was not discussed in this study because of the potential influence in the field and lab,
173 hence nine PAH compounds were discussed in this study.

174 Average recoveries of surrogate internal standards Acp-d10 and Phe-d10 were
175 61 ± 20 and 58 ± 21%. Five- or six-ring PAHs were not reported due to their low
176 recoveries (Chr-d12: 43 ± 15, and perylene-d12: 39 ± 17%), and most of them were
177 under the method detection limits. Although the polymeric sorbents produced lower
178 recoveries of the more volatile compounds, the C_{18} cartridge is considered a preferred
179 option for PAHs in water with good performance (Martinez et al., 2004). Sample
180 results were corrected for field blank values but not corrected for recoveries.

181 ### 2.4 Data Analysis

182 The statistical analysis was performed using SPSS (version 25). The
183 significant difference test was using the Mann-Whitney U test and Kruskal-Wallis
184 test, with p <0.05 indicating statistical significance. Principal component analysis
185 (PCA) was performed with varimax rotation, and principal components with
186 eigenvalues >1 were extracted. The calculation was performed using Microsoft Excel
187 (2019 Pro Plus), and figures were produced by software Ocean Data View (version
188 5.1.5) and Grapher (version 15.3.339).

189 Positive matrix factorization (PMF) analysis was performed using EPA PMF
190 5.0, and its concept and application have been described in detail in EPA PMF 5.0
191 Fundamental and User Guide (USEPA, 2014). The undetectable value was replaced
192 with one-half of its PAH method detection limits, and the uncertainty was set as 20%
193 for each PAH dataset. The model was run for 3–6 factors with random seeds, and the
194 output stability and reliability were checked according to Q value, residual analysis,
195 and correlation coefficients.

3 Results and Discussion

3.1 PAHs distribution in surface seawater

3.1.1 Concentration and sources

For surface seawaters collected from the Arctic and North Atlantic, the concentrations of 9 PAHs ($\sum_9$PAH) in the dissolved phase ranged from 0.3 to 10.2 ng L^{-1} (mean 4.3 ng L^{-1}) (Figure 2, Table S4). The average concentration of 9 PAHs in the Arctic Ocean (4.9 ± 2.8 ng L^{-1}) was higher than in the North Atlantic Ocean (3.4 ± 2.6 ng L^{-1}). The highest concentration was observed in the Barents Sea, near the Novaya Zemlya (AO04), while the lowest was found in the Norwegian Sea, North Atlantic (BB09). Three-ring compounds averagely contributed 86% to the total concentrations, among which Phe and Flu accounted for 34% and 31% of $\sum_9$PAH. PAH concentrations observed in this study were higher than those in the West Atlantic Ocean ($\sum_7$PAH: ND–8.1 ng L^{-1}, the concentrations were recalculated for our target compounds and the same below) (Lohmann et al., 2021) and North Atlantic Ocean ($\sum_7$PAH: 44–410 pg L^{-1}, Lohmann et al., 2009), lower than those in the Svalbard coastal ($\sum_7$PAH: ND–110 ng L^{-1}, Pouch et al., 2021) and the Pacific sector of the Arctic Ocean ($\sum_9$PAH: 23–51 ng L^{-1}, Na et al., 2021), and comparable to those in the Southern Ocean ($\sum_9$PAH: ND–6.3 ng L^{-1}, Cai et al., 2016), North Pacific Ocean ($\sum_7$PAH: 1.0–5.1 ng L^{-1}, Ke et al., 2017), and Japan Sea ($\sum_7$PAH: mean 5.4 ng L^{-1}, Chizhova et al., 2013). Details of the comparison with reported data are listed in Table S5.

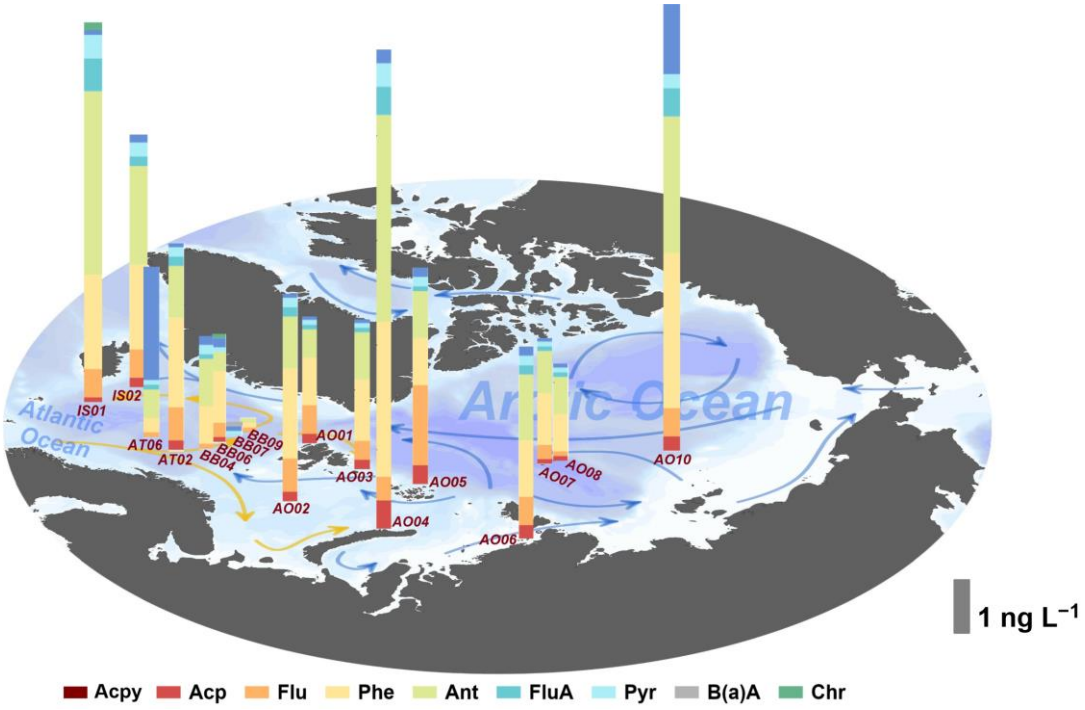

Figure 2. Spatial distribution of dissolved PAHs in the surface water from the North Atlantic Ocean and the Arctic Ocean.

Paired diagnostic ratios of certain individual PAHs have been widely used in the source estimation of PAHs (Yunker et al., 2002; Tobiszewski and Namiesnik, 2012). Considering PAHs in the dissolved phase dominated by low/medium molecule-weight compounds, we used FluA/(FluA + Pyr) and Ant/(Ant + Phe) to assess their possible sources. The FluA/(FluA + Pyr) ratio of less than 0.4 indicates a petrogenic source, and a value between 0.4 and 0.5 indicates mixed sources, while a value of more than 0.5 suggests a combustion source (Yunker et al., 2002). As shown in Figure S1, the FluA/(FluA + Pyr) ratios were mainly more than 0.4, implying that combustion and petroleum combustion were the major sources of PAHs in seawater. Besides, the ratio Ant/(Ant + Phe) could distinguish petrogenic and pyrogenic sources for PAHs (Yunker et al., 2002). Ant/(Ant + Phe) ratios, mostly more than 0.1, indicated the combustion source. It is worth noting that paired compounds usually have different reactivities to photodegradation and biodegradation, which may lead to a variance in the ratio value after long-range transport (Yunker et al., 2002; Liu et al., 2021b).

We further applied the PMF receptor model to estimate source profiles of PAHs in surface seawater by inputting 18 objects (samples), nine variables (PAHs), and their uncertainty data. Three factors were finally chosen according to Q robust and Q true values. The average contributions of nine PAHs to the three PMF factors are shown in Figure 3a, and these factor profiles are shown in Figure S2. Factor 1 made the least contribution (5%) to the total measured PAHs and was dominated by Pyr, a typical product of wood/coal combustion (Li et al., 2016). Factor 2 explained 15% of the PAH concentrations, with high loadings of Phe, Ant, FluA, BaA, and Chr. These PAH compounds have been regarded as typical products of wood/coal combustion and emission from gasoline and diesel vehicles, hence the profile of Factor 2 was indicative of combined combustion sources (Bzdusek et al., 2004; Zhang et al., 2021). Factor 3, accounting for the highest proportion (80%) of PAH concentrations, was mainly composed of Acpy, Acp, and Flu. This factor profile was of high consistency with PAH emission characteristics from gasoline and diesel combustion(Zeng et al., 2018). As shown in Figure S3, the PAH profile of the field blank showed some similarity to Factor 3, revealing the onboard contamination may partly come from the emission from the vessel’s diesel-based engines. It is worth noting that our limited input samples might lead to certain uncertainty in the PMF results. However, we suggested vehicle emissions and biomass combustion being the major PAHs sources in the surface seawater.

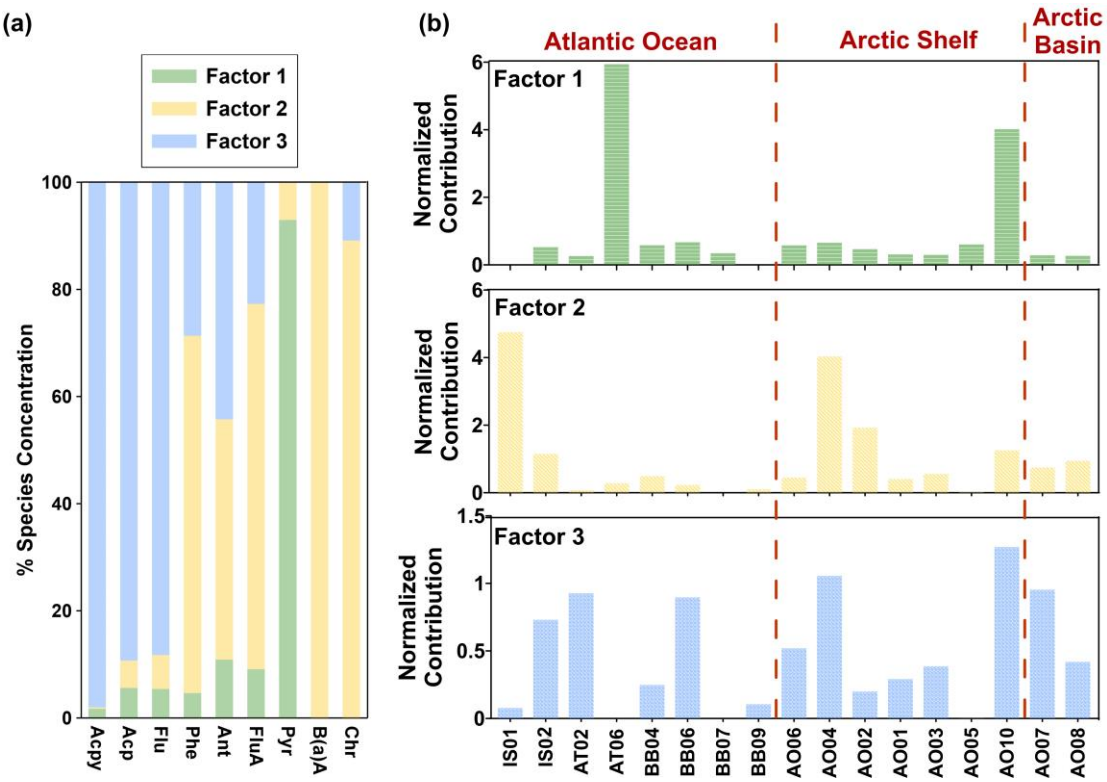

Figure 3. Results of the PMF model: (a) Source profiles of each PMF factor and (b) factor contribution to PAHs levels at each sampling site.

3.1.2 Distribution Patterns of PAHs

The spatial distribution of PAH concentrations in surface seawater showed an "Arctic Shelf > Atlantic Ocean > Arctic Basin" pattern, although the differences among these three areas were not statistically significant (p >0.05). The average $\sum_9$PAH concentrations were 5.5, 3.4, and 2.4 ng L^{-1} in the Arctic Shelf, the Atlantic Ocean, and the Arctic Basin. The average concentrations of 3-ring PAHs and FluA were highest in the Arctic shelf area (Figure S4), while the average concentrations of PAHs with higher molecular weights were highest in the Atlantic Ocean. The distribution of higher levels in the shelf area and lower levels in the basin area was similar to those of other SVOCs, such as PCBs and PBDEs (Carrizo et al., 2017). Previous studies have suggested the crucial role of long-range transport for SVOCs in high-latitude environments according to their latitudinal distribution (Lohmann et al., 2009; Zheng et al., 2021). However, no significant latitudinal trends were founded for individual PAHs or their sum concentrations (p: 0.156–0.902) except Chr (p <0.05), which indicates the local PAH input was also an important factor influencing their distribution trend. A significant decrease of PAHs was observed from the shelf area to the central basin of the Arctic Ocean (p <0.05), indicating a decreased input or enhanced depletion occurring in the upper ocean. Especially regarding the depletion mechanism, a strong particulate export could give rise to PAHs reducing during their lateral transport in the Arctic margins as the "shelf sink effect" (Liu et al., 2021a).

Regarding PAH compositions, only Acpy showed significant spatial distinctions (p <0.05). Figure 3b shows the relative contributions of PMF factors to $\sum_9$PAH levels in each surface seawater sample. Site AT06 in the Atlantic Ocean and site AO10 in the Arctic shelf were of the highest fraction of factor 1, while other samples were less impacted by factor 1. The fractions of factor 2 showed evident fluctuations in the Atlantic Ocean and the Arctic Shelf, with the highest value occurring at sites IS01 and AO04. As we previously discussed, factor 1 and factor 2 were representative of wood/coal combustion and vehicle emissions. Surface seawater in the Atlantic Ocean and Arctic Shelf areas were more impacted by wood/coal combustion and vehicle emissions, while they influenced the Arctic basin more evenly. Factor 3, regarded as a vehicle-emission source of PAHs, showed high fractions in these three areas such as AO07, AO10, and AT02. Therefore, land-based wood/coal combustion mainly impacted the Atlantic Ocean and Arctic Shelf areas, while vehicle emission from the terrestrial influenced the whole high-latitude areas.

The Arctic Ocean is surrounded by important source regions of PAHs (30% of the global emission), Eurasia, and North America, and is characterized by its broad continental shelf area and large river runoff (Gustafsson and Andersson, 2012). Atmospheric emissions of PAHs are expected to decrease by 46–71% and 48–64% in developed and developing countries before 2030 (Shen et al., 2013). However, as the most sensitive area to global warming, the Arctic is suggested to experience less magnitude of PAH decline according to modeling results (Balmer et al., 2019). Besides the re-volatilization of PAHs in the warming Arctic, recently increasing wildfires also lead to more PAH emissions to the atmosphere (Ma et al., 2011; McCarty et al., 2020). Therefore, we suggested that local inputs, such as snow/ice melting, permafrost thawing, and subsequent river runoff, were crucial for PAHs in the Arctic Ocean.

3.2 Depth profiles of PAHs in the water column

3.2.1 Hydrological Properties in the water column

The vertical profiles of temperature and salinity of seawater at sites AT06, BB04, IS02, and SR18 were shown in Figure 4, which generally represented the hydrological properties of the Greenland Sea, Norwegian Sea, and the central Arctic Ocean. Sectional distributions of temperature, salinity, dissolved oxygen, and fluorescence in the North Atlantic Ocean are shown in Figure S5.

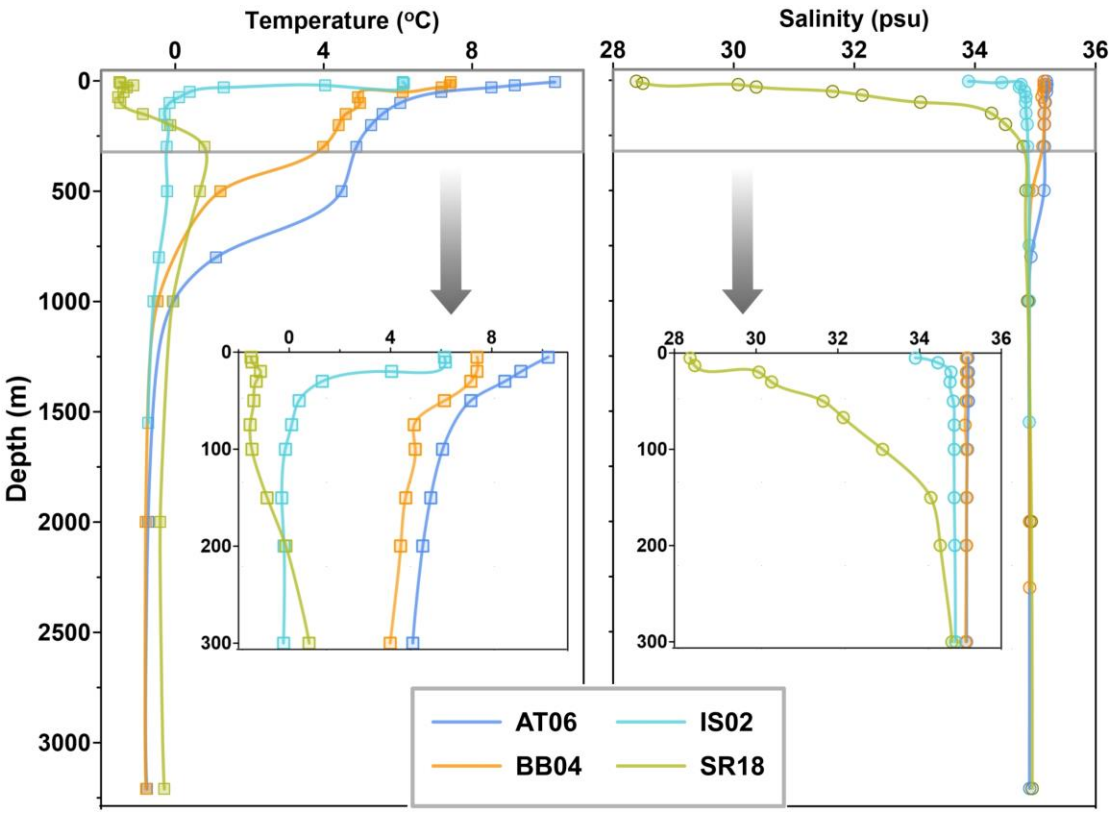

Figure 4. Vertical profiles of temperature and salinity of seawater at sites AT06, BB04, IS02, and SR18.

In the central Arctic Ocean (represented by SR18), there are generally three types of temperature-salinity relationships: low temperature with low salinity (Arctic Ocean Surface Water), low temperature with high salinity (Arctic Ocean Intermediate Water, Arctic Ocean Deep Water, and Bering Sea Deep Water), and high temperature with high salinity (Bering Sea Surface Water and Bering Sea Intermediate Water). As a result of riverine inflow, seasonal sea ice melting, and dense saline water from the Atlantic Ocean, the Arctic Ocean is strongly stratified. Its major water masses could be simply divided into Arctic Ocean Surface Water (<100 m), Arctic Ocean Intermediate Water (100–500 m), and Arctic Ocean Deep Water (Jakobsson, 2002).

In the Norwegian Sea (represented by AT06 and BB04) and Greenland Sea (represented by IS02), the differences in hydrological properties reflected water exchange between the Arctic Ocean and the North Atlantic Ocean. In the upper layer, the temperature and salinity of Atlantic seawater were higher than those in the central Arctic Ocean, with the highest value at AT06 (10.2°C). Seawater temperature showed a deeper mixing depth on the surface of the Norwegian Sea (100 m), followed by a sharp decrease at the 500–800 m depth layer. Seawater salinity showed higher values at the surface of the Norwegian Sea, while it was more stable in the deeper layer of the Greenland Sea. Water masses in the Norwegian Sea and the Greenland Sea are primarily divided into six classes, namely, surface water, Atlantic Water, dense

Atlantic Water, intermediate water, deep water I including Canadian Basin Deep Water and the lightest part of the Nordic Seas Deep Water, and deep water II including Eurasian Basin Deep Water and the deeper part of the Nordic Seas Deep Water (Rudels et al., 2005). Here we simply divided the water column in the North Atlantic Ocean into three layers: Modified North Atlantic Water (<800 m), Arctic Intermediate Water (800–1500 m), and Arctic Deep Water (>1500 m).

3.2.2 PAH profiles in water masses

In the water columns of the Greenland Sea, the Norwegian Sea, and the central Arctic Ocean, PAH concentrations ($\sum_9$PAH) ranged from 0.2 to 9.9 ng L^{-1}, with a mean value of 3.3 ng L^{-1} (Figure 5). The maximum concentration was found at a depth of 300 m at site SR18, near the north pole, and the minimum was located at 1000 m depth at site AT06 in the Norwegian Sea. PAHs in the water columns (Figure 5) showed a “surface-enrichment and depth-depletion” pattern similar to a previous study (Dachs et al., 1997). Specifically, PAHs were firstly enriched in the subsurface layer (50–300 m) with a mean value of 3.6 ng L^{-1}, after reaching a subsequent maximum at approximately 200–300 m depth, they eventually decreased and kept steady in the intermediate and deep water. For the component contribution, noticeable differences occurred among different water columns, while their variances with depth in one water column are not as noticeable. Such component coherence in one water column indicated, on an ocean scale, that PAHs are probably less influenced by the lateral transport compared with vertical transport processes.

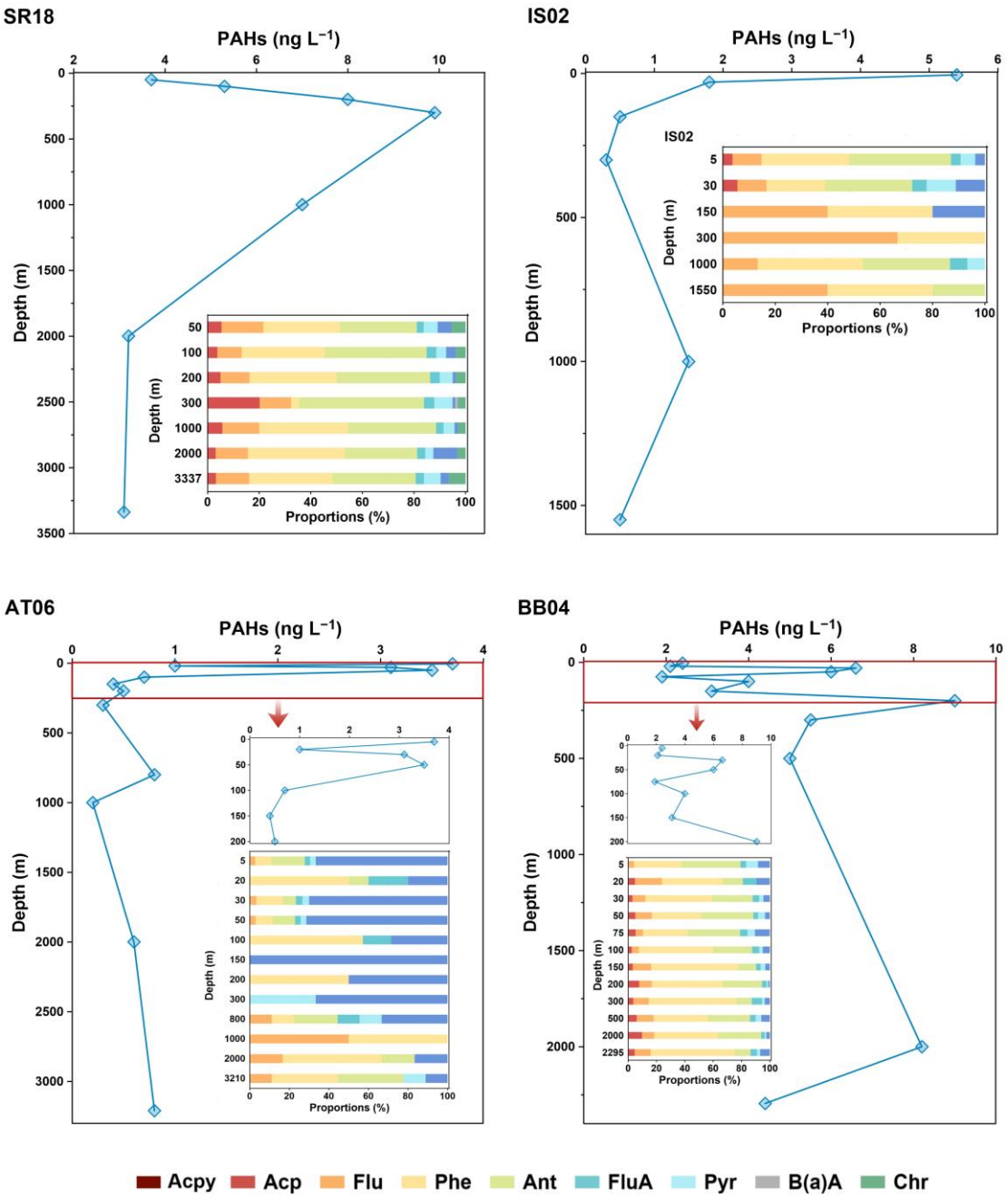

Figure 5. Vertical profiles of dissolved PAHs at sites SR18, IS02, AT06, and BB04.

The "surface-enrichment and depth-depletion" profile pattern reflected PAHs' biogeochemical processes occurring in the water column. Microbial degradation is considered the dominant depletion mechanism for dissolved PAHs in the open ocean, and this biodegradation process is weaker on the surface compared to the deep chlorophyll maximum (DCM) depth (González-Gaya et al., 2019). Taking the atmospheric input into consideration, it was reasonable to find the enrichment of PAHs at the surface. Besides, part of dissolved PAHs would partition to the particulate phase and subsequently sink to the deep-sea sediment, although the particulate-dissolved partitioning percentages (% on particles) were relatively low in the open ocean (Lohmann et al., 2021). As for the continental shelf, the flux of heat, freshwater, and nutrients through surrounding land has a significant effect on the thermohaline properties, giving rise to enhanced biological productivity (Krembs et al., 2011; Underwood et al., 2019). The dissolved organic carbon could further accelerate the photodegradation of small PAHs such as Phe by enhancing the formation of reactive intermediates (Shang et al., 2015). While in the intermediate and deep waters, where the primary productivity dropped, most dissolved PAHs are in low concentrations without considerable variations.

To further analyze PAH patterns in different water masses, we performed principal component analysis on individual PAH components after autoscaling the data, and three principal components (PCs) were derived from the analysis. The Keiser-Meyer-Olkin value of sampling adequacy was 0.703. PC1 contributed 41.4% to the total variance, heavily weighted in Flu, Phe, Ant, Acp, and FluA, mainly composed of three-ring PAHs with lower molecular weights. PC2, mainly composed of four-ring PAHs with higher molecular weights, contributed 25.9% to the total variance and is mainly weighted in BaA, Acpy, Chr, and FluA. PC3, explaining 11.7% of the total variance, was dominated by four-ring Pyr. We further divided seawater samples into four classes as surface and water-column samples in the Arctic Ocean and the North Atlantic Ocean (Figure 6). Their scores on PC1 and PC2 showed spatial variances at different depths, where PAHs in water columns showed higher loadings of PC2 (p <0.05). As four-ring PAHs are less biodegradable than three-ring PAHs, we suggested that the less degradable pattern of PAH compositions occurred in the deep layers.

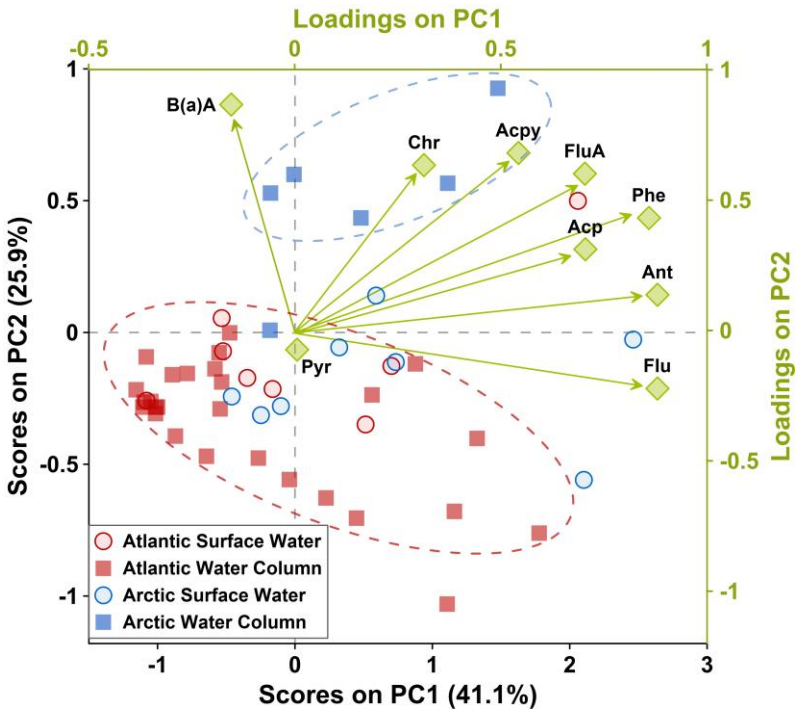

Figure 6. Results of principal compound analysis for PAHs in the Arctic Ocean and the North Atlantic Ocean.

3.3 Lateral transport of PAHs in the North Atlantic

3.3.1 Transport mass fluxes of PAHs

The lateral transport mass fluxes of PAHs through the Norwegian Atlantic Current and the East Greenland Current were estimated. The northward Norwegian Atlantic Current is characterized by the Atlantic Water (depth ≤840 m) and represented by seawater at AT06. The southward East Greenland Current is characterized by the Polar Water (depth ≤400 m) and represented by seawater at IS02. Assuming the diffusion fluxes were significantly less than the lateral transport, we estimated the mass fluxes (F, tons/year) for six frequently detected PAH compounds (Acp, Flu, Phe, Ant, FluA, and Pyr). Within a mass balance for lateral volume transport, the flux was estimated according to the water volume flux (V, Sv) and their depth-averaged concentration (C_{ave}, ng L^{-1}):

$$F = V \times C_{ave} \quad (1)$$

where we used the water volume fluxes based on long-term observation (Stöven et al., 2016). The annual average values of water volume fluxes are 4.4 ± 3.2 Sv and −1.4 ± 0.8 Sv for the Norwegian Atlantic Current and East Greenland Current, respectively. Recirculating Atlantic Water and Arctic Atlantic Water, whose volume fluxes are about −3.5 ± 1.9 Sv, were not discussed due to being indistinguishable in this study. Positive fluxes describe the northward fluxes into the Arctic Ocean, and negative values describe the southward fluxes from the Arctic Ocean (Stöven et al., 2016). The depth-averaged concentration (C_{ave}) was calculated using the trapezoidal integral equation (2):

$$C_{ave} = \frac{\int_{z=0}^{z=bottom} C_z d_z}{z_{bottom}} \quad (2)$$

where the bottom depths for the East Greenland Current and the Norwegian Atlantic Current were set as 300 m and 800 m, respectively. C_z is the PAH concentration at depth z according to the depth profiles of PAHs at AT06 and IS02.

As shown in Figure 7, PAH individuals' estimated transport mass flux ranged from 5.4 ± 3.9 to 58 ± 42 tons year^{-1} through the northward Norwegian Atlantic Current, with a sum of 110 ± 79 tons year^{-1}. The fluctuation of PAH individuals went from −1.6 ± 0.9 to −14 ± 8.0 tons year^{-1} through the southward East Greenland Current, with a sum of −45 ± 26 tons year^{-1}. For Flu, and Phe, mass flux values were close in different directions, while the mass flux was larger in the southward current for Acp but smaller for Ant, FluA, and Pyr. The net transport mass flux of PAH individuals ranged from −4.4 ± 1.7 to 53 ± 39 tons year^{-1} to the Arctic Ocean, with a sum of 63 ± 53 tons year^{-1}. It is worth noting that the estimation results were of certain error due to the seasonal variations. The transport volume has seasonal variations, with a maximum in March and a minimum in July, and the temperature of upper-layer waters also has strong seasonal signals (Beszczynska-Möller et al., 2012). Since the seawater samples were only collected during summer, the estimated annual flux was of uncertainty but provided the information on the magnitude of PAH transport flux.

Compared with the transport fluxes estimated for other POPs through the Fram Strait, PAH fluxes showed the same magnitude of HCHs, but a higher magnitude than PCBs and per- and polyfluoroalkyl substances (PFAS) (Ma et al., 2018; Joerss et al., 2020). Except for Acp, whose net flux value was negative, there were net inflows to the Arctic Ocean for the other 5 PAHs, and Pyr contributed the highest load (53 ± 39 tons year^{-1}), making up about 83% of the total mass flux. We found that with the increase of PAH molecular weight, the net mass flux to the Arctic Ocean increased. Previous studies reveal similar trends for PFAS, as a net outflow for shorter-chain PFASs and HCHs, while a net inflow for the PFASs with ≥ eight perfluorinated carbons or high-molecule weighted PCBs (Ma et al., 2018; Joerss et al., 2020).

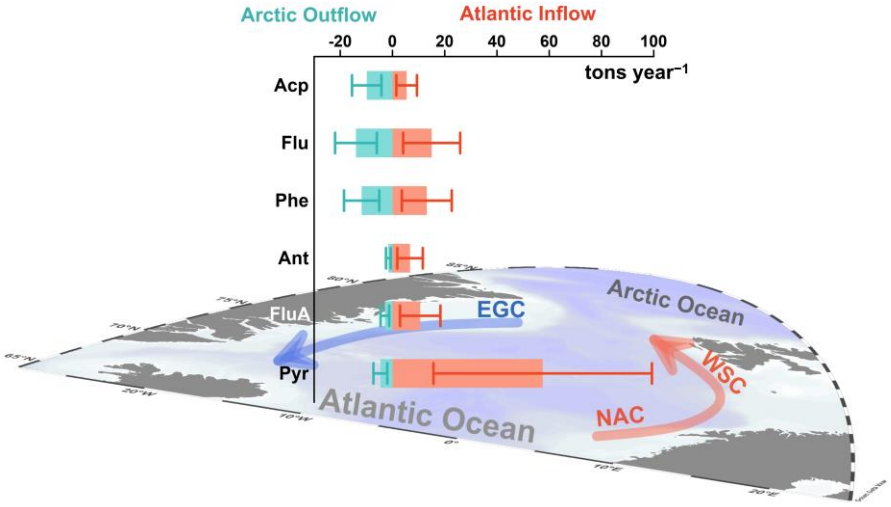

Figure 7. PAH mass transport through the northward Norwegian Atlantic Current (Atlantic inflow, positive value) and the southward East Greenland Current (Arctic outflow, negative value).

3.3.2 Contribution of oceanic transport for PAHs

The Arctic Ocean Boundary Current could be regarded as a relatively rapid and concentrated passage for Atlantic water to reach the western Arctic Ocean, with a larger spatial scale and more powerful driving force, while the discrete path of Pacific inflow in the Chukchi Sea slowed down the transit transport of Pacific water (Rudels et al., 1994; Mauldin et al., 2010). However, when comparing the oceanic transport with the atmospheric pathway, the latter has been considered a more efficient pathway for delivering pollutants to the Arctic, while the Atlantic oceanic transport was less important for PAHs in the seawater of Arctic fjords (Pouch et al., 2021). The oceanic advective time to the central basin is estimated to be years, while it takes only days for PAHs to arrive at the Arctic by air (Mauldin et al., 2010). Regarding the removal processes, including degradation and deposition/settling, they are usually slower in the seawater than in the atmosphere. The half-lives of PAHs in the oceans are usually in the order of tens or hundreds of days, while those in the atmosphere range from tens to thousands of hours (González-Gaya et al., 2019; Halsall et al., 2001; Liu et al., 2021a). Hence, the extent of PAH degradation or settling is expected to be higher during the oceanic transport to the Arctic, and we suggested that the ocean current was a less-dominant pathway for PAHs entering the Arctic Ocean.

The oceanic response to POPs change is slower but more complicated. Although the timescale of water mass transport is decades in the Atlantic and Arctic, which is longer than the half-lives of the dominant PAHs, oceanic fronts between two water masses could have an instantaneous effect on PAHs. Besides the direct delivery, the role of ocean currents should be further considered in their indirect impact on PAHs' air-sea interactions. Ocean currents could influence sea surface properties and the biogeochemical processes, subsequently modulating the air-sea exchange of PAHs (Lohmann and Belkin, 2014). To better understand the fate of POPs comprehensively, we suggest that further study should consider the oceanic modulations in both direct and indirect ways based on PAH data in multi-environments.

Conclusion

We investigated PAHs from surface seawater and full-depth water columns in the North Atlantic Ocean and the Arctic Ocean to better understand PAHs' transport processes and their contribution to high-latitude oceans. For surface seawaters collected from the Arctic and North Atlantic, the concentrations of 9 PAHs ($\sum_9$PAH) in the dissolved phase ranged from 0.3 to 10.2 ng L^{-1} (mean 4.3 ng L^{-1}). Their spatial distribution showed an "Arctic Shelf > Atlantic Ocean > Arctic Basin" pattern, and inputs from the surrounding margins were suggested to be crucial for PAHs in the Arctic Ocean. According to the results of PMF modeling, vehicle emissions and biomass combustion were the major sources of PAHs in the surface seawater. Besides, PAHs showed unique profiles indicating their different origins. Carried by East Greenland Current and the Norwegian Atlantic Current, PAH individuals' net transport mass flux ranged from -4.4 ± 1.7 to 53 ± 39 tons $year^{-1}$ to the Arctic Ocean, indicating ocean current was a less-dominant pathway for PAHs entering the Arctic Ocean. Although we suggested a limited contribution of

ocean currents on PAHs' delivery to the Arctic Ocean, their role in modulating PAHs' air-sea interactions and other biogeochemical processes needs further studies.

Acknowledgments and Data

We thank all the members of the Fifth Chinese National Arctic Research Expedition. This study was supported by National Natural Science Foundation of China (NSFC) (U2005207, 41976216, 41576180, 41776088, and 42106224), the Natural Science Foundation of Fujian Province, China (2014J06014), and China Scholarship Council (CSC) program (No.201806310096). We thank Ms. Mengxue Huang, Ms. Xuran Wang, Mr. Guangda Sun, and Mr. Mian Chen for their assistance during the experiments, thank Ms. Xuehong Zheng, Ms. Chunhui Wang, and Ms. Jun Ye for their help in lab management. There is no financial conflicts of interests for any author.

The sampling information, PAH data, calculation results and related figures are available in Spporting Information at Mendeley Data, Cai, Minggang (2021), "SI_PAHs in Arctic & Atlantic 2012", doi: 10.17632/fdd38cdtkj.1

References

Balmer, J. E., H. Hung, Y. Yu, R. J. Letcher, and D. C. G. Muir (2019), Sources and environmental fate of pyrogenic polycyclic aromatic hydrocarbons (PAHs) in the Arctic, *Emerging Contaminants*, *5*, 128-142, doi:10.1016/j.emcon.2019.04.002.

Beszczynska-Möller, A., E. Fahrbach, U. Schauer, and E. Hansen (2012), Variability in Atlantic water temperature and transport at the entrance to the Arctic Ocean, 1997–2010, *ICES Journal of Marine Science*, 69(5), 852-863, doi:10.1093/icesjms/fss056.

Bzdusek, P. A., E. R. Christensen, A. Li, and Q. Zou (2004), Source Apportionment of Sediment PAHs in Lake Calumet, Chicago: Application of Factor Analysis with Nonnegative Constraints, *Environmental Science & Technology*, *38*(1), 97-103, doi:10.1021/es034842k.

Cai, M., M. Liu, Q. Hong, J. Lin, P. Huang, J. Hong, J. Wang, W. Zhao, M. Chen, M. Cai and J. Ye (2016), Fate of Polycyclic Aromatic Hydrocarbons in Seawater from the Western Pacific to the Southern Ocean (17.5 ^{o}N to 69.2 ^{o}S) and Their Inventories on the Antarctic Shelf, *Environmental Science & Technology*, *50*(17), 9161-9168, doi:10.1021/acs.est.6b02766.

Carmack, E. C., M. Yamamoto-Kawai, T. W. N. Haine, S. Bacon, B. A. Bluhm, C. Lique, H. Melling, I. V. Polyakov, F. Straneo, M. L. Timmermans and W. J. Williams (2016), Freshwater and its role in the Arctic Marine System: Sources, disposition, storage, export, and physical and biogeochemical consequences in the Arctic and global oceans, *Journal of Geophysical Research: Biogeosciences*, *121*(3), 675-717, doi:10.1002/2015jg003140.

513 Carrizo, D., A. Sobek, J. A. Salvado, and O. Gustafsson (2017), Spatial Distributions of DDTs in the Water Masses
514 of the Arctic Ocean, *Environmental Science & Technology*, *51*(14), 7913-7919, doi:10.1021/acs.est.7b01369.

515 Chizhova, T., K. Hayakawa, P. Tishchenko, H. Nakase, and Y. Koudryashova (2013), Distribution of PAHs in the
516 northwestern part of the Japan Sea, *Deep Sea Research Part II: Topical Studies in Oceanography*, *86-87*, 19-24,
517 doi:10.1016/j.dsr2.2012.07.042.

518 Dachs, J., J. Bayona, C. Raoux, and J. Albaigés (1997), Spatial, Vertical Distribution and Budget of Polycyclic
519 Aromatic Hydrocarbons in the Western Mediterranean Seawater, *Environmental Science & Technology*, *31*, 682-
520 688, doi:10.1021/es960233j.

521 Dai, A., D. Luo, M. Song, and J. Liu (2019), Arctic amplification is caused by sea-ice loss under increasing CO_2,
522 *Nature Communications*, *10*(1), 121, doi:10.1038/s41467-018-07954-9.

523 Deyme, R., I. Bouloubassi, M.-H. Taphanel-Valt, J.-C. Miquel, A. Lorre, J.-C. Marty, and L. Méjanelle (2011),
524 Vertical fluxes of aromatic and aliphatic hydrocarbons in the Northwestern Mediterranean Sea, *Environmental*
525 *Pollution*, *159*(12), 3681-3691, doi:10.1016/j.envpol.2011.07.017.

526 Du, W., X. Yun, Y. Chen, Q. Zhong, W. Wang, L. Wang, M. Qi, G. Shen, and S. Tao (2020), PAHs emissions from
527 residential biomass burning in real-world cooking stoves in rural China, *Environmental Pollution*, *267*, 115592,
528 doi:10.1016/j.envpol.2020.115592.

529 González-Gaya, B., A. Martínez-Varela, M. Vila-Costa, P. Casal, E. Cerro-Gálvez, N. Berrojalbiz, D. Lundin, M.
530 Vidal, C. Mompeán, A. Bode, B. Jiménez and J. Dachs (2019), Biodegradation as an important sink of aromatic
531 hydrocarbons in the oceans, *Nature Geoscience*, *12*(2), 119-125, doi:10.1038/s41561-018-0285-3.

532 Gustafsson, Ö., and P. S. Andersson (2012), ^{234}Th-derived surface export fluxes of POC from the Northern Barents
533 Sea and the Eurasian sector of the Central Arctic Ocean, *Deep Sea Research Part I: Oceanographic Research*
534 *Papers*, *68*, 1-11, doi:10.1016/j.dsr.2012.05.014.

535 Halsall, C. J., A. J. Sweetman, L. A. Barrie, and K. C. Jones (2001), Modelling the behaviour of PAHs during
536 atmospheric transport from the UK to the Arctic, *Atmospheric Environment*, 35(2), 255-267, doi:10.1016/S1352-
537 2310(00)00195-3.

538 Hung, H., R. Kallenborn, K. Breivik, Y. Su, E. Brorström-Lundén, K. Olafsdottir, J. M. Thorlacius, S. Leppänen, R.
539 Bossi, H. Skov, S. Manø, G. W. Patton, G. Stern, E. Sverko and P. Fellin (2010), Atmospheric monitoring of
540 organic pollutants in the Arctic under the Arctic Monitoring and Assessment Programme (AMAP): 1993–2006,
541 *Science of The Total Environment*, *408*(15), 2854-2873, doi:10.1016/j.scitotenv.2009.10.044.

542 Jakobsson, M. (2002), Hypsometry and volume of the Arctic Ocean and its constituent seas, Geochemistry,
543 Geophysics, *Geosystems*, *3*(5), 1-18, doi:10.1029/2001GC000302.

544 Joerss, H., Z. Xie, C. C. Wagner, W.-J. von Appen, E. M. Sunderland, and R. Ebinghaus (2020), Transport of legacy
545 perfluoroalkyl substances and the replacement compound HFPO-DA through the Atlantic Gateway to the Arctic

Ocean—Is the Arctic a sink or a source?, *Environmental Science & Technology*, *54*(16), 9958-9967, doi:10.1021/acs.est.0c00228.

Ke, H., M. Chen, M. Liu, M. Chen, M. Duan, P. Huang, J. Hong, Y. Lin, S. Cheng, X. Wang, M. Huang and M. Cai (2017), Fate of polycyclic aromatic hydrocarbons from the North Pacific to the Arctic: Field measurements and fugacity model simulation, *Chemosphere*, *184*, 916-923, doi:10.1016/j.chemosphere.2017.06.058.

Keyte, I. J., R. M. Harrison, and G. Lammel (2013), Chemical reactivity and long-range transport potential of polycyclic aromatic hydrocarbons--A review, *Chem Soc Re*v, *42*(24), 9333-9391, doi:10.1039/c3cs60147a.

Ko, E., M. Y. Gorbunov, J. Jung, H. M. Joo, Y. Lee, K.-H. Cho, E. J. Yang, S.-H. Kang, and J. Park (2020), Effects of nitrogen limitation on phytoplankton physiology in the Western Arctic Ocean in Summer, *Journal of Geophysical Research: Oceans*, 1*25*(11), e2020JC016501, doi:10.1029/2020JC016501.

Krembs, C., H. Eicken, and J. W. Deming (2011), Exopolymer alteration of physical properties of sea ice and implications for ice habitability and biogeochemistry in a warmer Arctic, *Proceedings of the National Academy of Sciences*, *108*(9), 3653, doi:10.1073/pnas.1100701108.

Li, T., G. Sun, S. Ma, K. Liang, C. Yang, B. Li, and W. Luo (2016), Inferring sources of polycyclic aromatic hydrocarbons (PAHs) in sediments from the western Taiwan Strait through end-member mixing analysis, *Marine Pollution Bulletin*, *112*(1-2), 166-176, doi:10.1016/j.marpolbul.2016.08.024.

Liu, M., M. Chen, M. Duan, Y. Lin, X. Liu, J. Liang, H. Ke, H. Li, M. Chen, and M. Cai (2021a), Particulate Export of PAHs Firstly Traced by $^{210}Po/^{210}Pb$ Disequilibrium: Implication on the “Shelf Sink Effect” in the Arctic Ocean, *Journal of Geophysical Research: Oceans*, *126*(8), e2021JC017384, doi:10.1029/2021JC017384.

Liu, M., H. Zheng, W. Wang, H. Ke, P. Huang, S. Liu, F. Chen, Y. Lin, and M. Cai (2021b), Enhanced sinks of polycyclic aromatic hydrocarbons due to Kuroshio intrusion: Implications on biogeochemical processes in the ocean-dominated marginal seas, *Environmental Science & Technology*, *55*(10), 6838-6847, doi:10.1021/acs.est.1c01009.

Lohmann, R., and I. M. Belkin (2014), Organic pollutants and ocean fronts across the Atlantic Ocean: A review, *Progress in Oceanography*, *128*, 172-184, doi:10.1016/j.pocean.2014.08.013.

Lohmann, R., K. Breivik, J. Dachs, and D. Muir (2007), Global fate of POPs: Current and future research directions, *Environmental Pollution*, *150*(1), 150-165, doi:10.1016/j.envpol.2007.06.051.

Lohmann, R., R. Gioia, K. Jones, L. Nizzetto, C. Temme, Z. Xie, D. Schulz-Bull, I. Hand, E. Morgan, and L. Jantunen (2009), Organochlorine pesticides and PAHs in the surface water and atmosphere of the North Atlantic and Arctic Ocean, *Environmental Science & Technology*, *43*, 5633-5639, doi:10.1021/es901229k.

Lohmann, R., E. Markham, J. Klanova, P. Kukucka, P. Pribylova, X. Gong, R. Pockalny, T. Yanishevsky, C.C. Wagner, and E.M. Sunderland (2021), Trends of diverse POPs in air and water across the Western Atlantic Ocean: Strong gradients in the ocean but not in the air. *Environmental Science & Technology*, 55(14), 9498-9507, doi:10.1021/acs.est.0c04611.

Ma, J., H. Hung, C. Tian, and R. Kallenborn (2011), Revolatilization of persistent organic pollutants in the Arctic induced by climate change, *Nature Climate Change*, *1*(5), 255-260, doi:10.1038/nclimate1167.

Ma, Y., D. A. Adelman, E. Bauerfeind, A. Cabrerizo, C. A. McDonough, D. Muir, T. Soltwedel, C. Sun, C. C. Wagner, E. M. Sunderland and R. Lohmann (2018), Concentrations and water mass transport of legacy POPs in the Arctic Ocean, *Geophysical Research Letters*, *45*(23), 12972-12981, doi:10.1029/2018GL078759.

Ma, Y., Z. Xie, H. Yang, A. Möller, C. Halsall, M. Cai, R. Sturm, and R. Ebinghaus (2013), Deposition of polycyclic aromatic hydrocarbons in the North Pacific and the Arctic, *Journal of Geophysical Research: Atmospheres*, *118*(11), 5822-5829, doi:10.1002/jgrd.50473.

Mauldin, A., P. Schlosser, R. Newton, W. M. Smethie Jr., R. Bayer, M. Rhein, and E. P. Jones (2010), The velocity and mixing time scale of the Arctic Ocean Boundary Current estimated with transient tracers, *Journal of Geophysical Research: Oceans*, *115*(C8), doi:10.1029/2009JC005965.

McCarty, J. L., T. E. L. Smith, and M. R. Turetsky (2020), Arctic fires re-emerging, *Nature Geoscience*, *13*(10), 658-660, doi:10.1038/s41561-020-00645-5.

Morison, J., R. Kwok, C. Peralta-Ferriz, M. Alkire, I. Rigor, R. Andersen, and M. Steele (2012), Changing Arctic Ocean freshwater pathways, *Nature*, *481*(7379), 66-70, doi:10.1038/nature10705.

Na, G., J. Ye, R. Li, H. Gao, S. Jin, Y. Gao, C. Hou, and J. Huang (2021), Fate of polycyclic aromatic hydrocarbons in the Pacific sector of the Arctic Ocean based on a level III fugacity environmental multimedia model, *Marine Pollution Bulletin*, *166*, 112195, doi:10.1016/j.marpolbul.2021.112195.

Nizzetto, L., M. Macleod, K. Borgå, A. Cabrerizo, J. Dachs, A. D. Guardo, D. Ghirardello, K. M. Hansen, A. Jarvis, A. Lindroth, B. Ludwig, D. Monteith, J. A. Perlinger, M. Scheringer, L. Schwendenmann, K. T. Semple, L. Y. Wick, G. Zhang and K. C. Jones (2010), Past, present, and future controls on levels of persistent organic pollutants in the global environment, *Environmental Science & Technology*, *44*(17), 6526-6531, doi:10.1021/es100178f.

Pouch, A., A. Zaborska, M. Mazurkiewicz, A. Winogradow, and K. Pazdro (2021), PCBs, HCB and PAHs in the seawater of Arctic fjords – Distribution, sources and risk assessment, *Marine Pollution Bulletin*, *164*, 111980, doi:10.1016/j.marpolbul.2021.111980.

Rudels, B., G. Björk, J. Nilsson, P. Winsor, I. Lake, and C. Nohr (2005), The interaction between waters from the Arctic Ocean and the Nordic Seas north of Fram Strait and along the East Greenland Current: results from the Arctic Ocean-02 Oden expedition, *Journal of Marine Systems*, *55*(1), 1-30, doi:10.1016/j.jmarsys.2004.06.008.

Shang, J., J. Chen, Z. Shen, X. Xiao, H. Yang, Y. Wang, and A. Ruan (2015), Photochemical degradation of PAHs in estuarine surface water: effects of DOM, salinity, and suspended particulate matter, *Environmental Science and Pollution Research*, *22*(16), 12374-12383, doi:10.1007/s11356-015-4543-2.

Shen, H., Y. Huang, R. Wang, D. Zhu, W. Li, G. Shen, B. Wang, Y. Zhang, Y. Chen, Y. Lu, H. Chen, T. Li, K. Sun, B. Li, W. Liu, J. Liu and S. Tao (2013), Global atmospheric emissions of polycyclic aromatic hydrocarbons from

1960 to 2008 and Future Predictions, *Environmental Science & Technology*, *47*(12), 6415-6424, doi:10.1021/es400857z.

Sobek, A., and O. Gustafsson (2014), Deep water masses and sediments are main compartments for polychlorinated biphenyls in the Arctic Ocean, *Environmental Science & Technology*, *48*(12), 6719-6725, doi:10.1021/es500736q.

Steele, M., and T. Boyd (1998), Retreat of the cold halocline layer in the Arctic Ocean, *Journal of Geophysical Research: Oceans*, *103*(C5), 10419-10435, doi:10.1029/98JC00580.

Stemmler, I., and G. Lammel (2010), Pathways of PFOA to the Arctic: variabilities and contributions of oceanic currents and atmospheric transport and chemistry sources, *Atmospheric Chemistry and Physics*, *10*(20), 9965-9980, doi:10.5194/acp-10-9965-2010.

Stöven, T., T. Tanhua, M. Hoppema, and W. J. von Appen (2016), Transient tracer distributions in the Fram Strait in 2012 and inferred anthropogenic carbon content and transport, *Ocean Science*, *12*(1), 319-333, doi:10.5194/os-12-319-2016.

Talley, L. D., G. L. Pickard, W. J. Emery, and J. H. Swift (2011), Chapter 12 - Arctic Ocean and Nordic Seas, in Descriptive Physical Oceanography (Sixth Edition), edited by L. D. Talley, G. L. Pickard, W. J. Emery and J. H. Swift, pp. 401-436, Academic Press, Boston, doi:10.1016/B978-0-7506-4552-2.10012-5.

Tobiszewski, M., and J. Namieśnik (2012), PAH diagnostic ratios for the identification of pollution emission sources, *Environmental Pollution*, *162*, 110-119, doi:10.1016/j.envpol.2011.10.025.

Underwood, G. J. C., C. Michel, G. Meisterhans, A. Niemi, C. Belzile, M. Witt, A. J. Dumbrell, and B. P. Koch (2019), Organic matter from Arctic sea-ice loss alters bacterial community structure and function, *Nature Climate Change*, *9*(2), 170-176, doi:10.1038/s41558-018-0391-7.

USEPA (2014), EPA Positive Matrix Factorization (PMF) 5.0 Fundamentals and User Guide, edited. https://www.epa.gov/sites/default/files/2015-02/documents/pmf_5.0_user_guide.pdf.

Wang, P., W. Mi, Z. Xie, J. Tang, C. Apel, H. Joerss, R. Ebinghaus, and Q. Zhang (2020), Overall comparison and source identification of PAHs in the sediments of European Baltic and North Seas, Chinese Bohai and Yellow Seas, *Science of The Total Environment*, *737*, 139535, doi:10.1016/j.scitotenv.2020.139535.

Wang, X., J. Zhao, T. Hattermann, L. Lin, and P. Chen (2021), Transports and accumulations of Greenland Sea Intermediate Waters in the Norwegian Sea, *Journal of Geophysical Research: Oceans*, *126*(4), e2020JC016582, doi:10.1029/2020jc016582.

Xue, R., L. Chen, Z. Lu, J. Wang, H. Yang, J. Zhang, and M. Cai (2016), Spatial distribution and source apportionment of PAHs in marine surface sediments of Prydz Bay, East Antarctica, *Environmental Pollution*, *219*, 528-536, doi:10.1016/j.envpol.2016.05.084.

644 Yan, B., T. A. Abrajano, R. F. Bopp, D. A. Chaky, L. A. Benedict, and S. N. Chillrud (2005), Molecular tracers of
645 saturated and polycyclic aromatic hydrocarbon inputs into Central Park Lake, New York City, *Environmental*
646 *Science & Technology*, *39*(18), 7012-7019, doi:10.1021/es0506105.

647 Yeung, L. W. Y., C. Dassuncao, S. Mabury, E. M. Sunderland, X. Zhang, and R. Lohmann (2017), Vertical profiles,
648 sources, and transport of PFASs in the Arctic Ocean, *Environmental Science & Technology*, *51*(12), 6735-6744,
649 doi:10.1021/acs.est.7b00788.

650 Yu, Y., A. Katsoyiannis, P. Bohlin-Nizzetto, E. Brorström-Lundén, J. Ma, Y. Zhao, Z. Wu, W. Tych, D. Mindham,
651 E. Sverko, E. Barresi, H. Dryfhout-Clark, P. Fellin and H. HungYu (2019), Polycyclic Aromatic Hydrocarbons not
652 declining in Arctic air despite global emission reduction, *Environmental Science & Technology*, *53*(5), 2375-2382,
653 doi:10.1021/acs.est.8b05353.

654 Yunker, M. B., R. W. Macdonald, R. Vingarzan, R. H. Mitchell, D. Goyette, and S. Sylvestre (2002), PAHs in the
655 Fraser River basin: a critical appraisal of PAH ratios as indicators of PAH source and composition, *Organic*
656 *Geochemistry*, *33*(4), 489-515, doi:10.1016/S0146-6380(02)00002-5.

657 Zeng, Q., E. Jeppesen, X. Gu, Z. Mao, and H. Chen (2018), Distribution, fate and risk assessment of PAHs in water
658 and sediments from an aquaculture- and shipping-impacted subtropical lake, China, *Chemosphere*, *201*, 612-620,
659 doi:10.1016/j.chemosphere.2018.03.031.

660 Zhang, R., M. Han, K. Yu, Y. Kang, Y. Wang, X. Huang, J. Li, and Y. Yang (2021), Distribution, fate and sources
661 of polycyclic aromatic hydrocarbons (PAHs) in atmosphere and surface water of multiple coral reef regions from the
662 South China Sea: A case study in spring-summer, *Journal of Hazardous Materials*, *412*, 125214,
663 doi:10.1016/j.jhazmat.2021.125214.

664 Zhang, X., Y. Zhang, C. Dassuncao, R. Lohmann, and E. M. Sunderland (2017), North Atlantic Deep Water
665 formation inhibits high Arctic contamination by continental perfluorooctane sulfonate discharges, *Global*
666 *Biogeochemical Cycles*, *31*(8), 1332-1343, doi:10.1002/2017gb005624.

667 Zheng, H., M. Cai, W. Zhao, M. Khairy, M. Chen, H. Deng, and R. Lohmann (2021), Net volatilization of PAHs
668 from the North Pacific to the Arctic Ocean observed by passive sampling, *Environmental Pollution*, *276*, 116728,
669 doi:10.1016/j.envpol.2021.116728.